Composites Part B 106 (2016) 1–9

Contents lists available at ScienceDirect

Composites Part B

journal homepage: www.elsevier.com/locate/compositesb

Pulsed thermography inspection of adhesive composite joints: computational simulation model and experimental validation

Marcella Grosso [a, *], Juan E.C. Lopez [b], Vitor M.A. Silva [a], Sergio D. Soares [c], João M.A. Rebello [d], Gabriela R. Pereira [d]

[a] Laboratory of Non Destructive Testing, Corrosion and Welding (LNDC), Department of Metallurgical and Materials Engineering, Ferderal University of Rio de Janeiro, Rio de Janeiro, RJ, Brazil
[b] Physical Engineering Department, Science's School, EAFIT University, Medellín, Colombia
[c] Petrobras Research Center, Rio de Janeiro, Brazil
[d] Department of Metallurgical and Materials Engineering, COPPE/UFRJ—Federal University of Rio de Janeiro, P.O, CEP 21941-972, Rio de Janeiro, RJ, Brazil

ARTICLE INFO

Article history:
Received 2 May 2016
Received in revised form
26 July 2016
Accepted 4 September 2016
Available online 7 September 2016

ABSTRACT

We developed a computer simulation model using finite elements for the reproduction of physical phenomena found in active pulsed thermography of GFRP adhesive tubular joints. During the manufacture of the joint, defects such as the lack of adhesive were included in order to evaluate the ability of the active pulsed thermography technique to detect this type of material and joint configuration. The experimental results obtained with the thermographic camera were compared with a numerical approximation obtained through the simulation model developed in this study using the Comsol Multiphysics® software and, because of their similarity; it was possible to validate the computer simulation model. In both methods assessed in this study, it was only possible to detect the lack of adhesive when the thermographic test was performed from inside the joint, as, on the outer side of the joint, the defects' surfaces are at a depth greater than on the inner side.

1. Introduction

GFRP (Glass Fiber Reinforced Polymer) composites have been continuously employed in the oil industry in recent years, often on platforms, especially in pipes for water or oil transportation, under moderate temperatures, around 60 °C. Since pipelines transport fluids over long distances, joints have to be used to connect them. There are three main types of mechanical joints available for GFRP piping: concentric adhesive-bonded joints, laminated joints and threaded joints. Adhesive bonded joints and laminated joints are the most used ones as far as platforms are concerned.

During their manufacture, defects may appear in the adhesive layer, among which the most common ones are lack of adhesive and non-adherence. The presence of these defects on the joint compromises the integrity of the pipe, which can lead to risks of failure and severe damages to the environment. In view thereof, it is extremely important and necessary to search for non-destructive techniques capable of monitoring, evaluating and ensuring the integrity of these adhesive GFRP joints.

Over the past decades, the thermography technique has been used as a non-destructive technique for inspecting and detecting subsurface defects in composite materials. Pulsed thermography is the most common thermographic technique used. This technique consists of briefly heating the sample surface (varying from milliseconds for high conductivity materials to seconds for low conductivity materials), using an external pulsed heat source and, then, the surface temperature decay is recorded by an infrared camera. The presence of subsurface defects reduces the heat flow from the surface to the substrate, so, in the resulting thermal images, discontinuities appear as areas of different temperatures compared to the surrounding sound sample area. This is the principal mechanism to detect defective regions on thermal images [1–4]. When compared to other non-destructive techniques, thermography has the following advantages: no contact with the surface, fast inspection and easy interpretation of thermograms. In addition to these advantages, thermography is very successfully used in the inspection of high emissivity materials, such as composite materials.

There are some studies evaluating the capacity of thermography for inspection of composites, especially the GFRP [3,5,6] and CFRP

* Corresponding author.
E-mail address: marcellag@metalmat.ufrj.br (M. Grosso).

http://dx.doi.org/10.1016/j.compositesb.2016.09.011
1359-8368/

(Carbon Fiber Reinforced Polymer) [2,3,7,8]. However, the majority of studies were carried out on samples whose thickness was up to 6 mm and typically in thin plates. In the present work, an adhesive joint of GFRP will be used as a sample, whose thickness is 12 mm in order to investigate the detection limit on those structures. Therefore, this study brings some challenges related to depth of penetration of the thermal wave in the material to allow detection of defects and the uniformity of heat flux on the surface (because the curved shape of the joint).

There are few studies that use computational simulation to inspect composite materials through active thermography [9–15]. Vijayaraghavan et al. [16] in their study evaluated the capacity of flash thermography in detecting wall loss defects in thin cylindrical GFRP pipes using a numerical finite element method (FEM) to simulate the defects under 2D transient heat transfer. The study developed by Lopez et al. [17] proposes a methodology for the modelling and simulation of a pulsed thermography inspection of CFRP and additionally a parametric study was carried out in order to analyse the influence of the irradiation power density, non-uniform heating and characteristics associated with the defects.

As a result, the purpose of this study is to propose the creation of a model based on computer finite element simulation using Comsol Multiphysics® software to reproduce the physical phenomena present in the experiments through the use of active pulsed thermography in the adhesive joints of GFRP composites. The model developed in this study shows both the heating phase as the cooling phase of the material and a function was used to describe the incident energy on the material surface due to heat generated by the lamps. This model was validated and it is presented as a computer tool able to assess the ability to detect failures found in this type of joints and to establish and optimize the experimental parameters to be used by the active thermography technique during the relevant inspection.

2. Materials and methods

2.1. Test piece

To carry out the tests, a sample was prepared using a concentric adhesive bonded joint of GFRP. The sample is formed by two pipes,

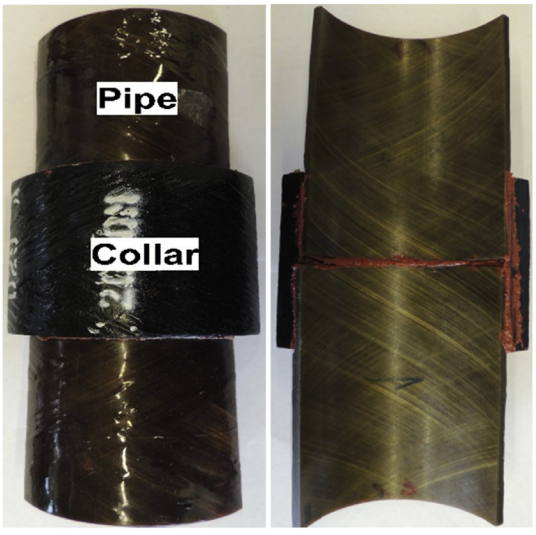

Fig. 1. Adhesive composite joint viewed from (a) outside and (b) inside.

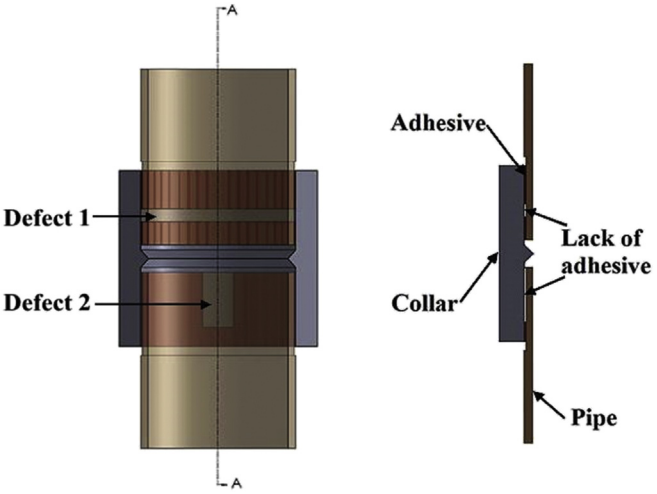

Fig. 2. Representation of the geometry and positioning of the two defects inserted in the adhesive layer.

with a diameter of 101.6 mm, thickness of 5 mm, joined trough a collar of 12 mm thickness, Fig. 1. An epoxy adhesive, with a thickness of 1 mm, was applied both over the collar's inner surface and over a surface of the pipes which was introduced into the collar. The two pipes were put together inside the collar similarly to a butt welded joint. For inspection purposes, the circumference of the joint was sectioned into three equal parts of 120°. The sample used in this work is shown in Fig. 1.

On the adhesive layer, some defects, as lack of adhesive, were inserted. This type of defect was introduced using thin polymer tapes, previously applied on the surface of the material in order to avoid that the adhesive would touch the surface of the pipe. After the application of the adhesive layer and before the adhesive cure, the tape was removed and then the adhesive was cured. Fig. 2 shows a representative scheme of the positioning of the two defects of lack of adhesive inserted in the adhesive layer of the joint. The defect 1 is located transversally to the pipe axis on the top of the joint has a width of 7.4 mm and extends from one end of the joint to the other end. The defect 2 is located along to the pipe axis at the bottom of the joint has a width of 18.4 mm and a length of 31.8 mm. Both defects have a thickness of 1 mm.

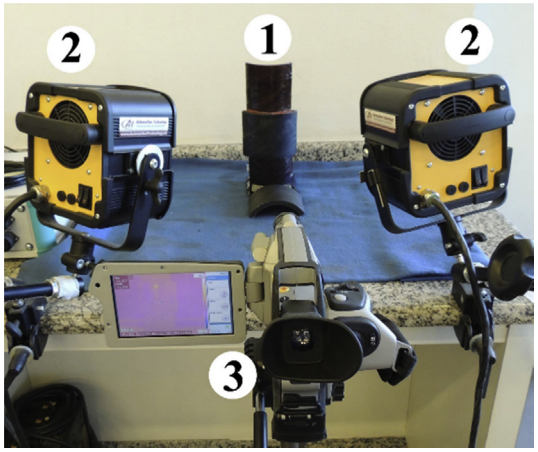

Fig. 3. Photography of the experimental set-up used in the thermographic tests (1 – sample, 2 – halogen lamps and 3 – infrared camera).

Table 1
Thermo-physical properties used for the pipe and the collar [18].

Material	Density, $\rho\left(\frac{kg}{m^3}\right)$	Heat capacity, C_p (*J/kg K*)	Thermal conductivity, k (W/m K)
Pipe/Collar	1800	910	0.33

2.2. Inspection of the specimen using pulsed thermography

Pulsed thermography was carried out with an infrared camera, which is an uncooled microbolometer Focal Plane Array (FPA) camera with a resolution of 640 × 480 pixels and with a thermal sensitivity of less than 0.06 °C. A set of 3.4 kW halogen lamps was used to generate a 30 s heat pulse on the material surface. The heat source was positioned on the same side of the specimen with respect to the IR camera (reflection mode). Fig. 3 shows a photography of the experimental set-up used in the thermographic tests.

The camera was controlled by a computer which allowed the capturing of thermal images with the same frame rate of the camera, 30 Hz, as well as the storage of these images.

2.3. Computational simulation of the physical phenomena

To reproduce the physical phenomena detected during the active pulsed thermography experiments, a Comsol Multyphisics® software, version 4.3, was used to create the simulation model and the default physical model heat transfer in solid module was used. A virtual solid was created to represent the 3D geometry of the sample used in this work with the inserted defects and their dimensions, as shown in Fig. 2.

For the simulation of heat transfer in the model, an equation which governs the heat transfer principle through conduction in transient state (Eq. (1)) was used:

$$\rho C_p \frac{\partial T}{\partial t} = \nabla \cdot (k \nabla T) + Q \tag{1}$$

where ρ is the material's density, C_p is the thermal capacity, k is the thermal conductivity of the material, T is the temperature, Q is the energy incident on the surface of the material and t is the time in seconds elapsed during the test.

To reproduce the adhesive joint with defects inserted in the adhesive layer, three materials were used in the model, namely: air, epoxy resin and the composite used in the pipe and in the collar of the joint. The thermal properties used in the physical equations for air and epoxy resin were obtained from the material library of the Comsol Multyphsics® software, through the selection of materials *air [gas]* and *filled epoxy resin*. However, the thermal properties related to the pipe and the collar of the joint were manually entered into the model by the user. Values used are shown in Table 1.

There are three principal boundary conditions on this model, which are defined by ambient temperature (T_{amb}=299.15 *K*) and the initial sample temperature (302.95 K) for the specific conditions of the laboratory's setup. The third boundary condition is the heat flow generated by the lamp as a result of the 30 s of heating during the thermographic test may be simulated through Eq. (2)

$$-n \cdot (-k \nabla T) = q_0 \tag{2}$$

where q_0 is the heat flow incident on the front surface of the joint exposed to the lamps during heating. To know the function that best represents the heat flow generated by the lamps used in the experimental apparatus, several simulations were performed with varying heat flow values for each heating time and the temperature of the surface obtained with the simulation was compared with the surface temperature of the sample obtained with the thermographic camera. After this analysis, the function that best reproduced the incident heat flow on the surface of the material generated by the lamp was obtained using the *piecewise cubic* interpolation and is presented in Fig. 4. In addition to being the model that is closer to the test reality, this kind of interpolation is also able to satisfy, with a good approximation, the cooling behaviour of the lamps immediately after the end of the heating period (behaviour observed from 30 s in the graph of Fig. 3).

During the material heating time, i.e., during the initial 30 s, during which lamps were on, the heat flow was of 5000 W/m^2 and after the heating (lamps switched off), the flow decreased to about 20 W/m^2 at the end of the 60 s of the test.

The emission of infrared radiation issued by the surface material was simulated by the following equation:

$$-n \cdot (-k \nabla T) = \varepsilon \sigma \left(T_{amb}^4 - T^4 \right) \tag{3}$$

where ε is the emissivity of the material, T_{amb} is the ambient temperature of the material and σ is the Stefan-Boltzmann constant (5.7×10^{-8} W m^{-2} K^{-4}). As the material used for this study was a GFRP composite, the emissivity value was set at 0.9, a value set in literature for composites containing glass fiber and polymer matrix [19].

Eq. (4) shows the equation used to simulate the convection cooling of the surface of the material exposed to heat and in contact with air

$$-n \cdot (-k \nabla T) = h \cdot (T_{amb} - T) \tag{4}$$

where h is the convective heat transfer coefficient in the air and which adopted value was of 20 W/m^{2}K [20].

In all cases, the values for each variable and physical property contained in Eqs (1)–(4) were given as parameters in the global definition of the model in Comsol Multyphisics®. In addition, all

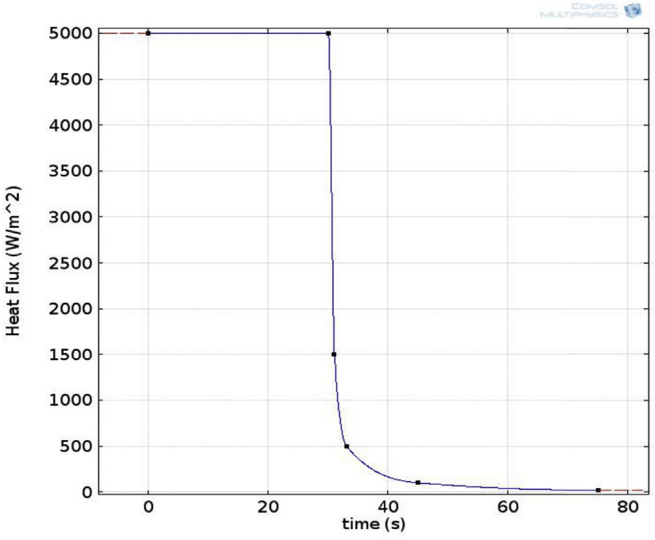

Fig. 4. Function which best represents the heat flow incident on the surface of the joint over time generated by the lamps.

Table 2
Mesh element size parameters.

Parameter	Size (pipe/collar)	Size (adhesive layer/defect)	Unit
Maximum element size	8	0.5	mm
Minimum element size	1	0.05	mm
Maximum element growth rate	2	1.8	–
Resolution of curvature	0.5	0.4	–
Resolution of narrow regions	0.6	0.6	–

simulations were developed in a 3D model and the mesh was created using tetrahedral elements due to this geometry can be adapted to any 3D volume and it use adaptive mesh refinement which was configured with the element size parameters described in Table 2. Fig. 5 shows the mesh in all the geometry space.

3. Results and discussion

In order to evaluate the influence of the thickness of the joint components in the detection of defects, tests were performed with the heating and analysis of data obtained by the thermographic camera both inside the joint (having the inner surface of the pipe sample as front side) and outside the joint (the external surface of the collar being the front side). The items below present the results for each side of inspection.

3.1. Heating and analysis from the outside of the joint

The first test was performed by placing the camera and lamps in front of the outer surface of the joint's collar (Fig. 6).

In order to have another tool to compare with the thermographic camera measurement, an array of LM35DZ temperature sensors in contact with the material surface was created to monitor the initial temperature of this surface prior to testing. The temperature was measured by a NI USB-6009 data acquisition board (DAQ) manufactured by National Instruments, responsible for converting the voltage generated by the sensors into digital data. The LabView® software was used to read these digital data and its subsequent conversion into graphs and tables with the temperature data.

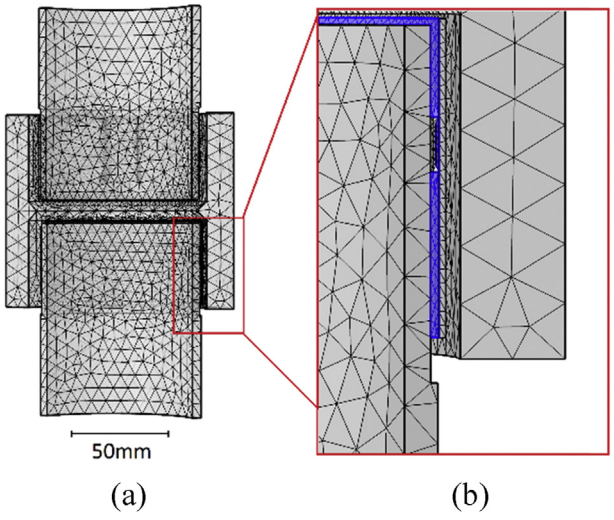

Fig. 5. The mesh applied in the sample: seen from the joint inside (a) and the mesh refinement in the region (blue) where defects were inserted in the adhesive layer in (b). (For interpretation of the references to colour in this figure legend, the reader is referred to the web version of this article.)

The result of the inspection was shown in a sequence of thermographic images, in which each frame showed the temperature distribution at the surface of the material at a certain time.

Fig. 7 shows the best thermal image obtained during the cooling of the joint without any image processing. The criterion for choosing the best image was based on the image that produced the highest thermal contrast between the defective region and the flawless region.

The same configuration adopted during the test described above was simulated in Comsol Multyphisics® using the model created for this study. The result of this simulation was recreated on images with the temperature distribution on the surface of the material over time. Fig. 8 shows the image of the external surface of the joint

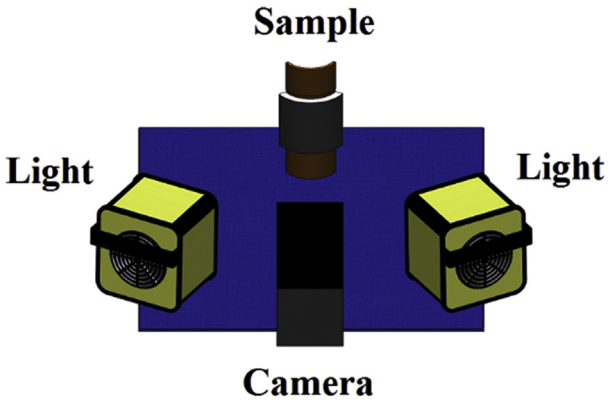

Fig. 6. Representative scheme of the camera and lamps positioning considering the analysis from the external surface of the joint.

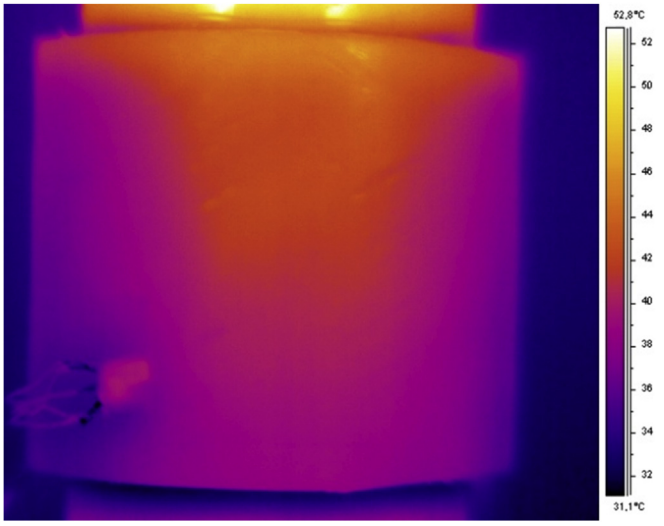

Fig. 7. Thermographic image at the time of the best contrast obtained through the thermographic inspection performed from the external side of the joint.

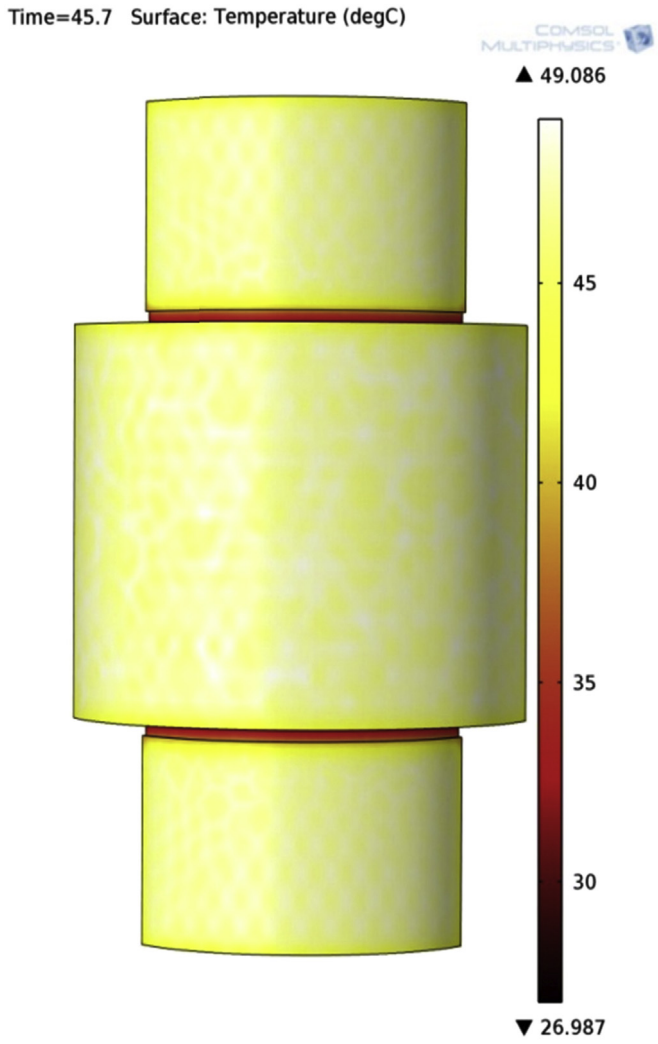

Fig. 8. Temperature distribution on the outer surface of the joint at the time of the best contrast obtained by the finite element simulation.

at the time of the best contrast obtained for the developed model.

By comparing the results obtained with the experimental method (Fig. 7) with the simulation (Fig. 8), we may see that, in both cases, the two defective regions inserted in the adhesive layer could not be detected.

The defects contained in the joint are not detected when the inspection is made from the external side of the joint, probably because of the great thickness of the collar (12 mm). Thermal wave has to penetrate this thickness to reach the adhesive layer where defects are inserted and show changes in the thermal contrast.

It is important to note that in the literature, studies developed using the pulsed thermography in composite materials (2, 5–17) were performed on materials whose maximum thickness is around 6 mm, unlike the present study, in which the thickness of the collar is 12 mm. Thus, the present study aimed to evaluate thicknesses until now unexplored in the literature to determine the defect detection limit to the depth in this type of material.

3.2. Heating and analysis from the inside of the joint

By performing the thermographic inspection from inside the joint, i.e., the inner surface of the pipe sample (Fig. 9), it is possible to see in the original thermographic image (Fig. 10) two lighter

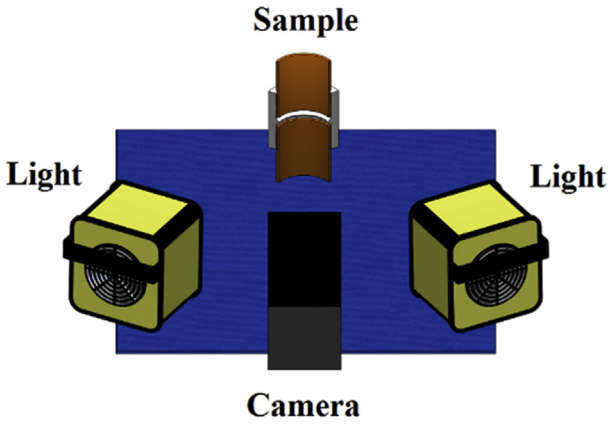

Fig. 9. Representative scheme of the camera and lamps positioning considering the analysis from the internal surface of the joint.

regions, i.e. regions with temperatures above the rest of the joint. The first region highlighted in the thermographic images is located in the upper part of the joint and extends horizontally from one end of the joint to the other end, corresponding to the defect 1 previously inserted in the material according to the diagram in Fig. 2. However, there are some vertical stripes next to the defect 1 that in fact correspond to the reflection effect of light waves generated by the lamps on the surface of the sample, and not to defects since they are not uniform throughout the sequence of images analysed in the test, a behaviour that differs from the defective regions. The second region in the image is located at the bottom of the joint and extends vertically from the center to the edge of the joint; this region coincides with the region in which the defect 2 of lack of adhesive was inserted, according to the scheme of Fig. 2.

Fig. 11 shows the thermal image shown in Fig. 10 converted into an 8 bit grayscale (scale from 0 (black) to 255 (white)) for the analysis of the distribution of grey levels in the two defective areas detected. For this analysis, we used the image processing software Image-PRO® in the *Line Profile* function. In each one of the defective areas detected, a line was positioned to analyse the distribution of grey levels over all pixels contained in this line, Fig. 11. Fig. 12 shows the line profile obtained for the horizontal defect in the upper part of the joint (Line 1) and Fig. 13 shows the profile obtained for the vertical defect at the bottom of the joint (Line 2). By analysing both

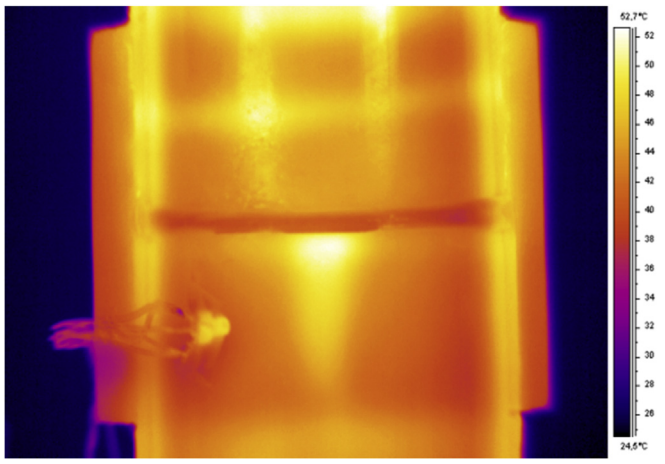

Fig. 10. Thermographic image at the time of the best contrast obtained through the thermographic inspection performed from the internal side of the joint.

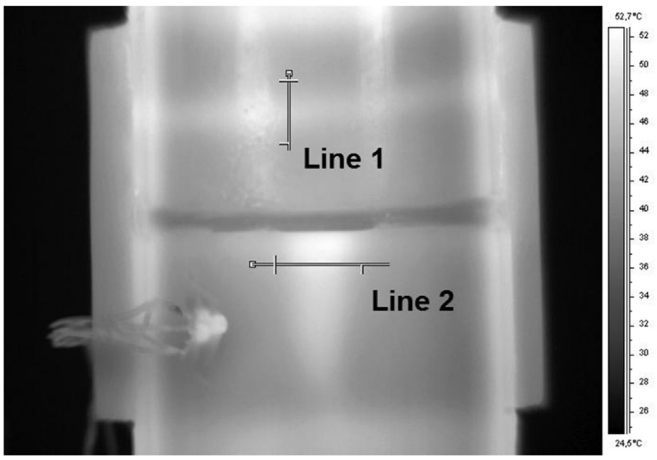

Fig. 11. Thermographic image converted into an 8-bit grey scale illustrating the position of lines in the defective areas detected.

profiles obtained (Figs. 12 and 13), it is possible to see that the grey intensity of pixels located in the region of the defects increases. This behaviour can also be explained by Fig. 11, in which the regions of the defects have higher temperatures (pixels are clearer based on the scale used, i.e. higher values in the grey scale) than the region without any defects (pixels have a darker shade according to the adopted scale, i.e. lower values in the grey scale).

Fig. 14 shows the image of the best thermal contrast of the temperature distribution on the inner surface of the joint obtained by simulating the model created by adopting the same configuration used in an experimental test. It is possible to see that the two defects (defect 1 and defect 2) were detected in the simulation with a high level of thermal contrast, i.e., there is a large temperature difference in these two regions if compared to the joint region without defect, a fact that enables the detection of these regions.

As the inspection is carried out inside the joint, by comparing the results obtained by the simulation of the created model and by the experimental method, it is possible to observe that, in both, the two defects of lack of adhesive entered were detected. However, the resulting image of the computer simulation shows the contours of the defects in higher definition than the image obtained by the experimental method, since, in the simulation, all physical phenomena are reproduced under optimal testing conditions and since external factors that influence the test and that cannot be measured are eliminated. In addition, the reflection of the lamps presented in the images resulting from the experimental method is a parameter which cannot be easily reproduced in the computer simulation.

Another aspect that should be highlighted in the analysis of the results obtained refers to the limit of detection found during the inspection of this joint using the active thermography technique. When the inspection is performed from the outside of the joint, the depth that the thermal wave has to penetrate in the material until it

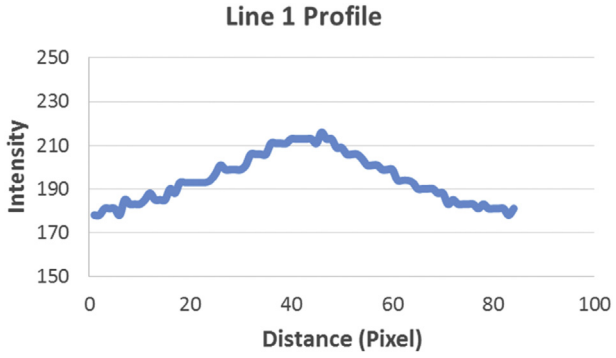

Fig. 12. Grey level profile along the pixels in line 1 (Line1) relative to the horizontal defect located on the top of the thermographic imaging.

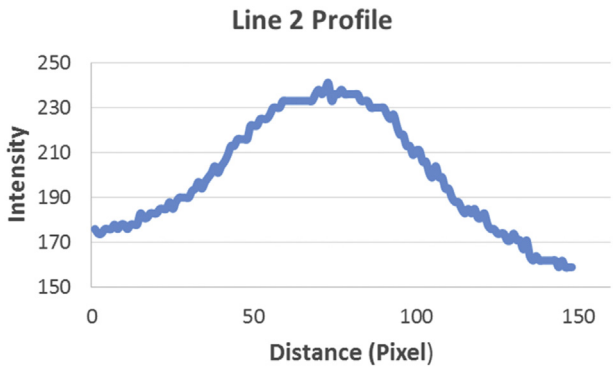

Fig. 13. Grey level profile along the pixels in line 2 (Line2) relative to the vertical defect located on the bottom of the thermographic imaging.

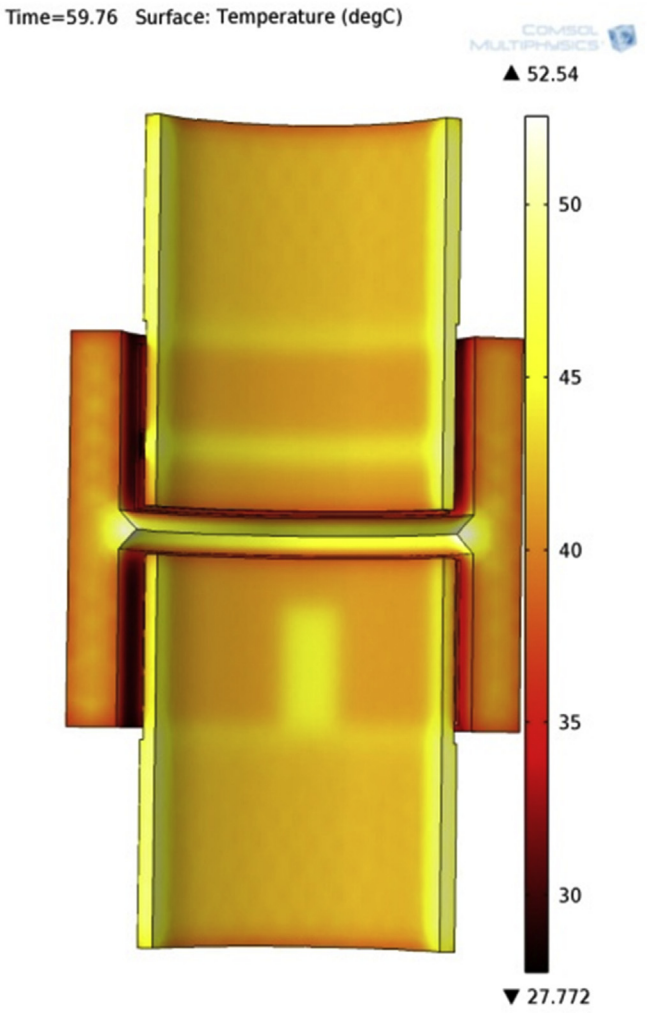

Fig. 14. Temperature distribution on the inner surface of the joint at the time of the best contrast obtained by the finite element simulation.

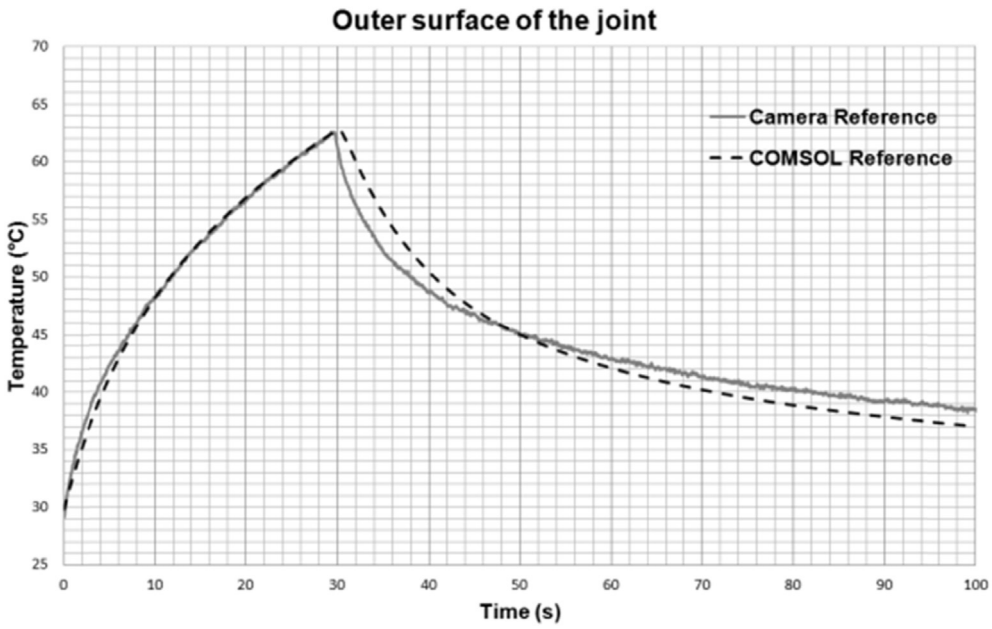

Fig. 15. Comparison of results obtained using the experimental method and the simulation for the external joint surface.

finds the defect is around 12 mm, this thickness is related to the coupler/collar, and in this inspection configuration, no defect was detected during the test or simulation. However, when inspection is made from inside the joint, the thickness required for the thermal wave to penetrate the material until it reaches the defect is of around 6 mm; this thickness refers to the pipe sample and the adhesive layer, and in this configuration, both methodologies detected both defects in the joint.

The result obtained when an inspection is carried out inside the joint is considered very interesting, since in the literature the pulsed thermography is employed for inspection of low thicknesses composite material (usually below 6 mm). With the results obtained in this study, it can be established that the limit of detection in this material is deeper than the depths studied in the literature. For example, in the study by Vijayaraghavan et al. [12], in which a GFRP pipe of 6 mm thickness containing wall loss defects localized at different depths, the results indicated that only defects with depths less than 3 mm could be detected using flash thermography, while in this work, the defect of lack of adhesive was detected at a depth of 6 mm from the inspected surface.

Thus, it can be said that the defect detection limit in this type of material, under these test conditions, is between 6 mm and 12 mm, but further studies must be performed in order to find the thickness limit to detect defects, such as the lack of adhesive, in this type of

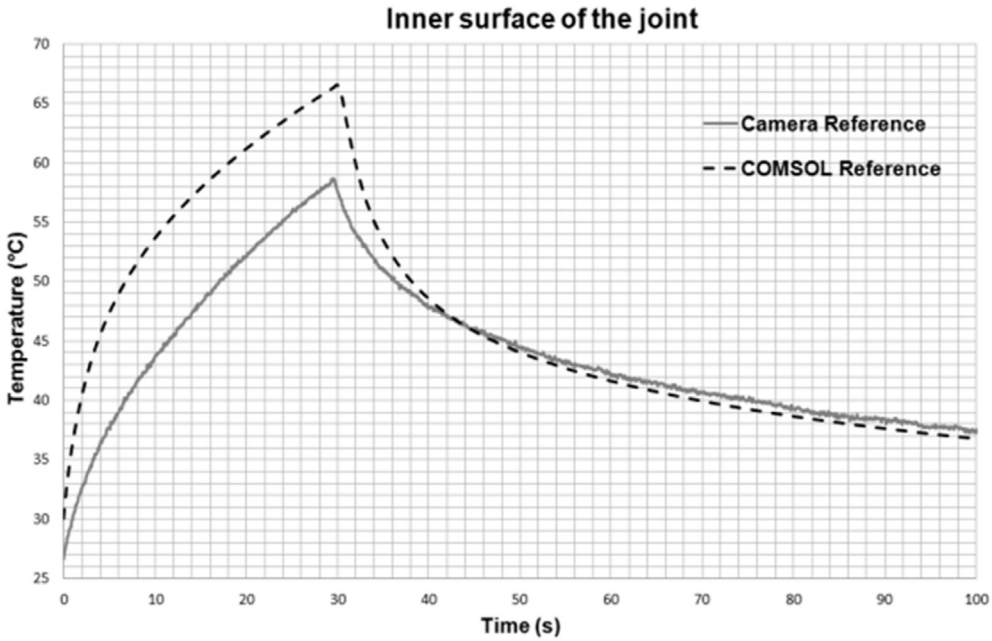

Fig. 16. Comparison of results obtained using the experimental method and the simulation for the internal joint surface.

joint, using the active thermography technique.

3.3. Comparison of results (numerical simulation and experimental)

Although the results of the finite element simulation of the model developed in this study were similar to those obtained with the experimental method, as far as the detection of the defects inserted into the joint is concerned, a behavioural analysis of temperature data for each of the methodologies evaluated in this study was also carried out.

In a certain area on the outer surface of the joint, the temperature data collected by the thermographic camera over time were compared with the data obtained in the same area for the simulated model, according to the graph shown in Fig. 15. In the graph analysis, it is possible to see that, during the 30 s of material heating, the difference between the two temperature curves is extremely small in average (approximately 1 °C), i.e., the error obtained in the finite element simulation of the thermal behaviour on the collar surface compared with the actual behaviour provided by the thermographic camera was very small. However, during the material cooling phase, after 30 s of heating, the difference between the values obtained for each method was slightly higher than in the heating phase, but this difference still remained small, since, in the simulated model, physical phenomena and the test conditions are reproduced under ideal conditions while during the experimental test, there is an external influence that, even if not measured, can cause a deviation from the ideal behaviour.

In the case of the inspection performed on the inner side of the joint, by comparing the temperature data obtained for each method, Fig. 16, it was possible to see that the temperature curve obtained with the simulated model showed a moderate difference in relation with the curve with experimental temperature data during the heating of the material surface. However, during the cooling phase, after the 30 s of heating, the difference between the temperature curves obtained for the experimental test and the simulated model was very small, around 2 °C. Please note that during the cooling phase, there is a better contrast between the defective area and the sound area of the material and even with a moderate difference between the two curves during the heating phase, it is the cooling phase which becomes more important for the analysis of detection of defects and at, this stage, the difference between the temperature data obtained for the two methods was similar [1].

The inspection from inside is important to discover if with a smaller thickness is possible to detect the defects. The actual conditions of use of this type of joints in oil platforms, they could be found with 4-inch diameter (as the case of our study) or in larger diameters.

Based on these results, we may say that the finite element model presented results close to the experimental data, a fact which validates this model developed to simulate the thermographic test in these types of composite joints.

4. Conclusion

This study proposed the creation of a model through computer finite element simulation for the reproduction of the experimental active pulsed thermography test in the adhesive joints of GFRP composites with some defects inserted on the adhesive layer.

The model created in this study describes the test by thermography in transient regime completely, both in heating and in cooling, unlike other studies published that are focused only on cooling analysis. Additionally, in this model was inserted a function that describes the energy incident on the surface of the material during the test (heating and testing), and this function was found by doing several experimental tests.

According to the settings used in the equipment, parameters related to the material evaluated in this study and the type of the defect (lack of adhesive), as described in item 2, the experimental results demonstrated that, when the inspection was performed using thermography on the outside of the joint (collar), it was not possible to detect the presence of defects of lack of adhesive in the thermographic images. However, when the inspection was performed within the joint, the two defects of lack of adhesive were detected. This behaviour is related to the depth of the defects in relation to the surface being inspected by the technique.

By comparing the results for the two methods evaluated in this study, the model developed by computer simulation proved to be reliable and useful in relation to the reproduction of physical phenomena involved in the experiments.

The creation of a model by computer simulation able to reproduce the experimental test can reduce the time spent preparing the experimental test, as well as figuring out the best parameters to be used for inspection. In addition to this, with the validation of the model created in this study, it will be possible to estimate the detection limit found in the inspection of composite joints using the active thermography technique.

Based on the results obtained in this study, the limit for detecting defects such as the lack of adhesive found during the inspection using active pulsed thermography in adhesive bonded joints is in the thickness range of 6–12 mm, in the conditions presented in this paper.

Considering that other settings, both for the specimen and the adopted experimental parameters, can change this thickness range found as detection limit, further tests should be performed regarding the use of optimized parameters for thermographic inspection in order to find out the detection thickness limit.

Acknowledgements

Authors would like to acknowledge the sponsorship of PETROBRAS, the Brazilian research agencies CNPq (Brazilian National Council for Scientific and Technological Development) and CAPES (Coordination for the Improvement of Higher Education).

References

[1] Maldague XPV. Infrared and thermal testing – non destructive testing. ASNT; 2001.
[2] Pickering SG, Almond DP. Matched excitation energy comparison of the pulse and lock-in thermography NDE techniques. NDT&E Int 2008;41:501–9.
[3] Brown JR, Hamilton HR. Quantitative infrared thermography inspection for FRP applied to concrete using single pixel analysis. Construct Build Mater 2013;38:1292–302.
[4] Maldague XPV. Theory and practice of infrared technology for nondestructive testing. New York: John-Wiley & Sons; 2001.
[5] Harizi W, Chaki S, Bourse G, Ourak M. Mechanical damage assessment of glass fiber-reinforced polymer composites using passive infrared thermography. Compos Part B Eng 2014;59:74–9.
[6] Lobonati F, Vergani L. Damage assessment of composite materials by means of thermographic analyses. Compos Part B Eng 2013;50:82–90.
[7] Alexis C, Franck B, Didier D, Emmanuel A, Hangseok C. Evaluation of gluing of CFRP onto concrete structures by infrared thermography coupled with thermal impedance. Compos Part B Eng 2015;69:350–8.
[8] Zheng K, Chang Y, Yao Y. Defect detection in CFRP structures using pulsed thermographic data enhanced by penalized least squares methods. Compos Part B Eng 2015;79:351–8.
[9] Krishnapillai M, Jones R, Marshall IH, Bannister M, Rajuc N. Thermography as a tool for damage assessment. Compos Struct 2005;67:149–55.
[10] Krishnapillai M, Jones R, Marshall IH, Bannister M, Rajic N. NDTE using pulse thermography: numerical modelling of composite subsurface defects. Compos Struct 2006;75:241–9.
[11] Almeida RM, Souza MPC, Rebello JMA. Defect detection in composite coatings by computational simulation aided thermography. Rev Prog Quant Nondestruct Eval 2010;29:1127–34.

[12] Hain M, Bartl J. Active thermography as a method for non-destructive testing. In: Measurements and applications. SPIE; 2012. p. 7746.
[13] Ptaszek G, Cawley P, Almond D, Pickering S. Transient thermography testing of unpainted thermal barrier coating (TBC) systems. NDT&E Int 2013;59:48–56.
[14] Krishnapillai M, Jones R, Marshall IH, Bannister M, Rajic N. Thermography as a tool for damage assessment. Compos Struct 2005;67:149–55.
[15] Vijayaraghavan GK, Sundaravalli S. Evaluation of pits in GRP composite pipes by thermal NDT technique. J Reinf Plastics Compos 2011;30(19):1599–604.
[16] Vijayaraghavan GK, Sundaravalli S. Numerical modelling and analysis of wall loss defects in thin cylindrical GRP pipes using flash thermography. e-Journal of Non Destruct Test; 2011. http://www.ndt.net/article/ndtnet/2011/34_Vijayaraghavan.pdf [accessed 29.03.16].
[17] Lopez F, Nicolau VP, Ibarra-Castanedo C, Maldague X. Thermal-numerical model and computational simulation of pulsed thermography inspection of carbon fiber-reinforced composites. Int J Therm Sci 2014;86:325–40.
[18] AMERON. Bondstrand® product guide: bondstrand® 2000, 4000 and 7000 glassfiber reinforced epoxy (GRE) pipe systems for general service. 2012.
[19] Öhman Claes. Emittance measurements using AGEMA E-Box. Technical report. AGEMA; 1999.
[20] Incropera FP, De Witt DP. Introduction to heat transfer. 2nd ed. New York, NY: John Wiley & Sons; 1990.